TISSUE ENGINEERING: Part A
Volume 19, Numbers 3 and 4, 2013

DOI: 10.1089/ten.tea.2011.0738

Full-Thickness Skin Wound Healing Using Human Placenta-Derived Extracellular Matrix Containing Bioactive Molecules

Ji Suk Choi, PhD,[1,2,*] Jae Dong Kim, MS,[1,2,*] Hyun Soo Yoon, PhD,[3] and Yong Woo Cho, PhD[1,2]

The human placenta, a complex organ, which facilitates exchange between the fetus and the mother, contains abundant extracellular matrix (ECM) components and well-preserved endogenous growth factors. In this study, we designed a new dermal substitute from human placentas for full-thickness wound healing. Highly porous, decellularized ECM sheets were fabricated from human placentas via homogenization, centrifugation, chemical and enzymatic treatments, molding, and freeze-drying. The physical structure and biological composition of human placenta-derived ECM sheets dramatically supported the regeneration of full-thickness wound *in vivo*. At the early stage, the ECM sheet efficiently absorbed wound exudates and tightly attached to the wound surface. Four weeks after implantation, the wound was completely closed, epidermic cells were well arranged and the bilayer structure of the epidermis and dermis was restored. Moreover, hair follicles and microvessels were newly formed in the ECM sheet-implanted wounds. Overall, the ECM sheet produced a dermal substitute with similar cellular organization to that of normal skin. These results suggest that human placenta-derived ECM sheets provide a microenvironment favorable to the growth and differentiation of cells, and positive modulate the healing of full-thickness wounds.

Introduction

Skin is the largest organ of the human body and plays a crucial role in many functions, such as protection against microorganisms, maintaining body temperature, and providing sensory information about the external environment.[1] Damage to the integrity of the skin caused by genetic disorders, acute trauma, chronic wounds, or surgical procedures may result in significant disability or even death. Most wounds can heal naturally, but full-thickness wounds greater than 1 cm in diameter need a skin graft to prevent scar formation, resulting in impaired morbidity and cosmetic deformities.[2] To enhance the restoration of a full-thickness cutaneous wound and to improve the quality of wound healing, several kinds of skin substitutes, such as autografts, allografts, xenografts, and tissue-engineered skin products, have been developed, some of which are commercially available for clinical use. However, there are still considerable problems, including limited supply, high manufacturing costs, excessive inflammation, various disease risks, and the quality of wound healing, which give rise to the clinical need for more advanced alternatives.[3] Recently, interest in biological scaffolds derived from decellularized tissues or organs has grown rapidly for use as surgical implants and scaffolds for regenerative medicine because extracellular matrix (ECM) secreted from resident cells of each tissue and organ can provide a favorable microenvironment that affects cell migration, proliferation, and differentiation.[4–6]

Herein, the human placenta is presented as a dermal substitute for the reconstitution of full-thickness wounds. The placenta is a complex organ that facilitates the physiological exchange between the fetus and the mother and has an extremely rich reservoir of ECM and bioactive molecules.[7] In the whole placenta, including the amnion, which contain collagen (types I, IV, VII, and XVII), elastin, laminin, proteoglycans, and adhesion proteins, play an important role in the maintenance of vessel walls and villous integrity.[8] Moreover, many growth factors secreted from the mother during pregnancy, such as insulin-like growth factor-1 (IGF-1), epidermal growth factor (EGF), platelet-derived growth factor (PDGF), fibroblast growth factor-2 (FGF-2), vascular endothelial growth factor (VEGF), and transforming growth factor-β (TGF-β), are delivered to the fetus through the placenta, suggesting that they have important roles in promoting the growth of the developing fetus.[9] Furthermore, the biological properties of the placenta, such as anti-inflammatory, antibacterial, low immunogenicity, antiscarring, and wound protection, make it an

Departments of [1]Chemical Engineering and [2]Bionanotechnology, Hanyang University, Ansan, Republic of Korea.
[3]Department of Chemical and Biological Engineering, Seokyeong University, Seoul, Republic of Korea.
*These two authors contributed equally to this work.

ideal candidate to treat burned skin, leg ulcers, and ophthalmic disorders.[10–13]

The human placenta can be harvested without harm to the donor and are commonly discarded. The matrix components of the placenta are similar to those of the skin and several growth factors in the placenta are involved in wound healing and angiogenesis. Therefore, the compositional and biological properties of the placenta have the potential to provide a highly favorable environment for wound healing. In this study, we prepared a decellularized ECM sheet with a variety of well-preserved proteins and bioactive molecules from the placenta, and explored the potential of human placenta-derived ECM sheets for use in full-thickness wound healing through *in vivo* experiments. We expected that human placenta-derived ECM sheets could provide not only structural guidance for cell behaviors, but also mechanical and chemical cues for full-thickness wound healing.

Materials and Methods

Preparation of decellularized ECM from human placentas

Five human placentas were obtained with informed consent from normal or Caesarean deliveries at the Hanyang University Medical Center after ethical approval. The placenta was washed several times with distilled water to remove blood components. Distilled water was added to the placenta and the tissue/water mixture (2:1) was homogenized for 5 min at room temperature using a blender (Shinil Industrial Co.). The placenta extracts (ECM) were centrifuged at 3000 *g* for 5 min, and the upper layer containing the blood residue was discarded. The ECM suspension was washed several times and centrifuged at 3000 *g* for 5 min. Subsequently, the ECM suspension was treated with a buffered 0.5% sodium dodecyl sulfate (SDS; Sigma) (diluted 1:1) for 30 min at room temperature in a shaking water bath (Taitec). The ECM suspension was centrifuged and rinsed with distilled water for 4 days at room temperature under shaking until residual SDS was removed. The suspension was then treated with a mixture of 0.2% DNase (2000 U; Sigma) and 200 μg/mL RNase (Sigma) for 10 min at 37°C. The final products were centrifuged and thoroughly washed with distilled water for 2 days. The final ECM and distilled water were homogeneously mixed in the proportion of 2:1 (v/v), and then the decellularized ECM was gently poured into a round-shaped mold, frozen at −70°C, and freeze-dried for at least 48 h. Decellularized ECM sheets (15-mm diameter and 10-mm thickness) were sterilized by ethylene oxide gas and hydrated with 10 mL phosphate-buffered saline for 5 min before *in vivo* implantation.

DNA quantification

DNA was isolated with a commercial extraction kit (G-spin Kit; iNtRON Biotechnology). The total DNA content was measured by absorption at 260 nm on a spectrophotometer (NanoDrop 1000; Thermo Fisher Scientific). All samples were normalized to the ECM or placenta dry weight.

Biochemical analyses

Biochemical assays were performed to quantify the ECM components, such as acid/pepsin-soluble collagen, sulfated glycosaminoglycan (GAG), and soluble elastin.[14,15] Sircol acid/pepsin-soluble collagen, Blyscan sulfated GAG, and Fastin elastin assay kits (Biocolor) were used according to the manufacturer's protocol. For extraction of acid/pepsin-soluble collagen, samples were digested with 0.5 M acetic acid containing 1% (w/v) pepsin (Sigma) at room temperature for 24 h. The digested suspension was centrifuged and the supernatant was incubated with 1 mL Sircol dye reagent for 30 min at room temperature. For extraction of sulfated GAG, samples were digested with 0.1 M phosphate buffer (pH 6.8) containing 125 μg/mL papain (Sigma), 10 mM cystein hydrochloride (Sigma), and 2 mM ethylenediaminetetraacetic acid (Sigma) at 60°C for 48 h. The supernatant was mixed with 1 mL Blyscan dye and the precipitate was collected via centrifugation. For extraction of elastin, ECM was hydrolyzed with 0.25 M oxalic acid (Sigma) at 100°C for 50 min.[16] The insoluble residues were separated by centrifugation and soluble elastin was mixed with 1 mL Fastin dye. The relative absorbance was measured in a 96-well plate using a microplate spectrophotometer (BioTek Instruments). All contents were normalized to the ECM or placenta dry weight in milligrams. Collagen type I (rat tail), chondroitin 4-sulfate (bovine trachea), and α-elastin (bovine neck) were used as standards for the biochemical assays.

Cytokine array and quantitative analysis of growth factors

Bioactive molecules in the placenta (100 mg) and decellularized ECM (100 mg) were analyzed using a cytokine antibody array kit (RayBiotech) according to the manufacturer's protocol. The placentas and decellularized ECMs obtained from five donors were dissolved in the basal buffer (50 mM Tris-HCl, pH 7.4 and 0.1× protease inhibitor) containing 2 M urea at 4°C for 3 days. The mixture was centrifuged at 1000 *g* for 30 min at 4°C to remove insoluble materials and the supernatant was collected. The array glass chip containing 80 different human cytokine antibodies was blocked and incubated with ECM extract. The glass chip was washed and subsequently treated in biotin-conjugated antibodies. After incubation with fluorescent dye-conjugated streptavidin, cytokine signals were detected by a laser scanner (Axon Instruments) using the Cy3 channel. Signal intensities were quantified with GenePix Pro software. For quantification of the growth factors present in the extraction solution, enzyme-linked immunosorbent assay (ELISA) was performed using TGF-β1, bFGF, EGF, PDGF, IGF-1, and VEGF ELISA kits (Koma Biotech) according to the manufacturer's protocol. The optical density was then measured at 450 nm using a microplate spectrophotometer (BioTek Instruments).

Scanning electron microscopy and porosity measurement

The microstructures of the ECM sheets were observed by scanning electron microscopy (SEM) (Tescan). The specimens were fixed using a 2.5% glutaraldehyde solution for 20 min, dehydrated through a series of graded ethanol solutions, and then lyophilized overnight. The samples were observed using SEM after being coated with platinum by sputtering at an accelerating voltage of 15 kV. The pore size and porosity of

the ECM sheets (2.5-cm diameter and 1.5-cm thickness) were determined using an automated mercury porosimeter (Micromeritics).

Tensile testing

Tensile tests were conducted with a universal tensile machine equipped with a 200 N static load cell (Instron). A specimen (20-×5-×1-mm, length×width×thickness) was pulled at a rate of 2.54 mm/min. Strains were calculated by cross-head displacement, and stresses were calculated by dividing force data by the cross-sectional area of the sample. Five specimens were measured and averaged.

Full-thickness cutaneous wound models

Thirty-six rats divided into two groups were wounded, and then implanted with or without a human placenta-derived ECM sheet. Under general anesthesia, the dorsal area was completely depilated, and a full-thickness circle wound (about 169 mm^2 in area) was created in the upper back area of each rat (female, Sprague-Dawley rat, weighting 80–120 g; HanaBio). Wounds were wrapped with plastic molds for protection. At 1, 2, and 4 weeks after treatment, six rats treated with ECM sheets and six control rats were sacrificed, and the skins, including wounds, were harvested for histological examination. The cutaneous wounds were photographed, and the wound areas were measured based on the image produced by the Imaging Analyzer (Bio-Rad Laboratories).

Histological and immunofluorescence examinations

Specimens were fixed in 4% paraformaldehyde, embedded in paraffin, and sliced at 6–10-μm thickness using a microtome. The sections were deparaffinized and dehydrated through a series of graded ethanol. Hematoxylin and eosin (H&E) staining was used to detect the presence of residual nucleated cells or cell fragments, and 4,6-diamidino-2-phenylindole (DAPI; Thermo Scientific) staining was used to identify nuclear components. For collagen and elastic fiber staining, sections were stained with Gomori's trichrome and orcinol-new fuchsin solution, respectively. To visualize re-epithelialization and vascularization in an implanted ECM sheet, sections were incubated with a 10% (w/v) bovine serum albumin blocking agent for 30 min to inhibit nonspecific binding of immunoglobulin G (IgG). Sections were incubated with mouse anti-human collagen I (Santa Cruz Biotechnology), rabbit anti-rat collagen I (Abcam), mouse anti-rat laminin 5 (Santa Cruz Biotechnology), goat anti-rat loricrin (Santa Cruz Biotechnology), and mouse anti-rat PECAM-1 (Santa Cruz Biotechnology) and detected with fluorescein-conjugated rabbit anti-goat or bovine anti-mouse IgG (Santa Cruz Biotechnology). Sections were counterstained with 1 μg/mL DAPI for 1 min. All of the stained sections were observed with a fluorescence microscope (Olympus).

Statistical analysis

Experimental data are expressed as means ± standard deviation. The Student's two-tailed *t*-test with SPSS 17.0 statistical software (SPSS) was used for comparison, and statistical significance was accepted at $p < 0.05$.

Results

Preparation of decellularized human placenta-derived ECM

Following a modified procedure,[17] ECM was isolated from whole human placentas (Fig. 1A, B). Human placentas were washed several times with distilled water to remove blood components. ECM was extracted from the placenta via homogenization, centrifugation, SDS, and nuclease treatments. The mean yield of final dry ECMs was approximately 441 mg/g of dry human placenta ($n = 5$). The effective removal of the cells and nucleic acids from the ECM was confirmed using H&E and DAPI staining (Fig. 1C–F). In the native placenta, abundant cell components and nucleic acids were apparent. However, after the decellularization, cells and nucleic acids were hardly observed in ECM. The dsDNA in ECM was also quantified. Compared to the native human placenta (772.0 ± 224.04 ng/mg placenta), the dsDNA content of decellularized ECM (34.3 ± 13.2 ng/mg ECM) was significantly reduced (Fig. 1G).

Composition analysis

The placenta, which supplies oxygen and nutrients from the mother to the fetus, is a rich source of ECM and bioactive molecules.[9] To analyze ECM components after decellularization, biochemical assays (Fig. 2A) and histological staining (Fig. 2B) were performed. The native placenta was rich in collagen (391 ± 18 μg/mg), elastin (425 ± 25 μg/mg), and sulfated GAG (47 ± 4 μg/mg). After decellularization, the human placenta-derived ECM still retained large amounts of collagen (315 ± 21 μg/mg) and elastin (324 ± 77 μg/mg). A small amount of sulfated GAG (20.9 ± 0.6 μg/mg) was also found. Gomori's trichrome and orcinol-new fuchsin staining also revealed that collagen and elastin appeared to be preserved after decellularization.

Endogenous bioactive molecules in the ECM were arrayed on a glass chip containing 80 different cytokine antibodies. The tissue lysate from the placenta was used as a control. Among the 80 bioactive molecules, 27 types of cytokines related to a cellular immune response and 25 types of growth factors related to cell growth and differentiation were detected in the ECM, as shown in Figure 3A and B. Notably, several growth factors known to be regulators of wound healing were detected at a high level of expression in the decellularized ECM, such as TGF-β1 (114 ± 49 pg/mL), bFGF (1385 ± 323 pg/mL), EGF (193 ± 14 pg/mL), PDGF (202 ± 19 pg/mL), IGF-1 (846 ± 186 pg/mL), and VEGF (87 ± 36 pg/mL), although the contents of growth factors in the decellularized ECM were decreased compared with those of the native placenta (TGF-β1, 137 ± 15 pg/mL; bFGF, 2092 ± 275 pg/mL; EGF, 424 ± 29 pg/mL; PDGF, 256 ± 13 pg/mL; IGF-1, 1118 ± 302 pg/mL; VEGF, 219 ± 127 pg/mL) (Fig. 3C).

Physicomechanical properties of decellularized ECM sheets

The extracted ECM was fabricated into porous sheets through molding and freeze-drying (Fig. 4A). The ECM sheets (13-mm diameter and 1-mm thickness) possessed a highly porous microstructure with a high degree of interconnectivity (Fig. 4B). The mean pore size was 62.21 μm and

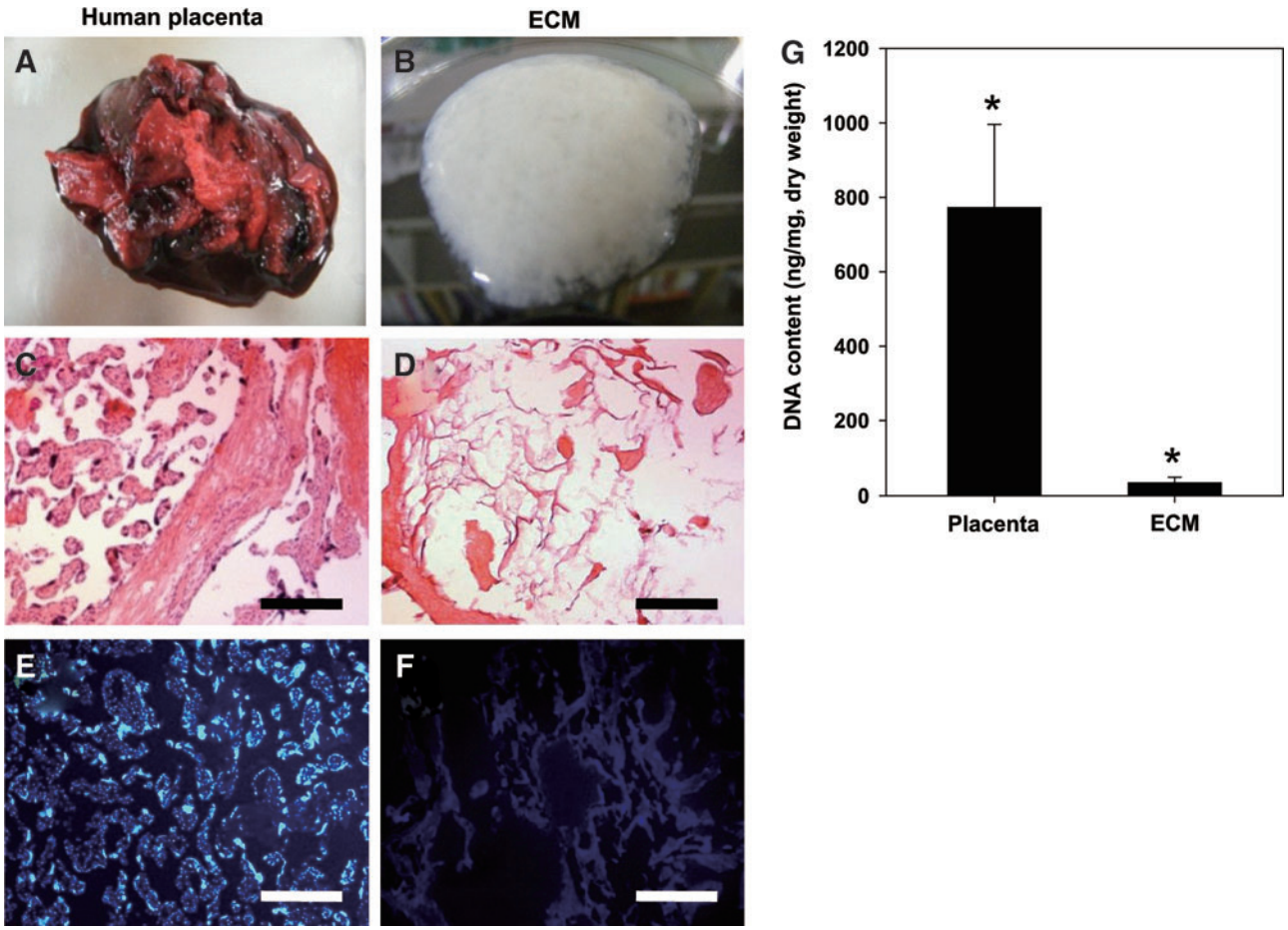

FIG. 1. Preparation of decellularized human placenta-derived ECM. **(A, B)** ECM was extracted from human placenta and decellularized through physical, chemical, and enzymatic treatment. **(C, D)** Cell cytoplasm (pink) and nuclei (dark purple spot) in decellularized ECM were stained with H&E. **(E, F)** Nucleic acids were also stained using DAPI that binds strongly to A-T-rich regions in DNA. Scale bars represent 200 μm. **(G)** DNA contents in human placenta and ECM. Samples were normalized to the ECM dry weight. Data are shown as mean ± standard deviation ($n = 5$) with significance at $^*p < 0.05$. ECM, extracellular matrix; H&E, hematoxylin and eosin; DAPI, 4,6-diamidino-2-phenylindole. Color images available online at www.liebertpub.com/tea

the average porosity was 99.54%, which is sufficient for cell infiltration, transport of nutrients, and gas exchange (Fig. 4C). The ECM sheet had a tensile strength of 0.052 MPa (Fig. 4D). Most naturally derived biomaterials have a viscoelastic property and show a wide range of strength values, such as collagen fibers of cartilage (1–7 MPa), collagen gels of calf skin (0.001–0.009 MPa), heart muscles of rats/humans (0.003–0.07 MPa), and skin of rat (6.58–9.52 MPa).[18,19] The results observed in the mechanical testing suggest that the decellularized placenta-derived ECM sheet has appropriate mechanical characteristics for use as a skin substitute.

Effect of an ECM sheet on the full-thickness wound healing

Figure 5A shows the wound healing process after treatment with an ECM sheet and without it. During the first day postoperation, the ECM sheet efficiently absorbed wound exudates and tightly attached to the wound surface. At 1 week postoperation, scabs were observed in both groups. It is notable that the wounds of the control group were greatly reduced in size. At 2 weeks postoperation, the scabs were falling off the wounds, and the wounds were mostly filled with restored skin. Complete wound closure was observed in both groups at 4 weeks. The restored skin treated with an ECM sheet was similar to normal skin, while an elongated scar was still observed in the healed skin of a control group due to excessive contraction. The wound images were quantified to show the healing areas at different time points. As shown in Figure 5B, the difference between the control group and the ECM sheet group was remarkable at 1 week after the operation ($p < 0.05$), but was not significant at 2 or 4 weeks.

Histological and immunofluorescence staining were used to assess the wound-healing processes and the structure of the restored tissues (Figs. 6 and 7). One week after the operation, the control and the ECM sheet-implanted groups exhibited abundant inflammatory cells. The wounds in the control group were distinguishable from adjacent tissues, and no clear keratin layer was observed. In the ECM sheet-implanted group, new epidermic cells had migrated around the wound edge and a keratin layer was clearly observed. After 2 weeks, the wound size in the control group decreased faster than in an ECM sheet group, but re-epithelialization and keratinization were incomplete. On the other hand, the

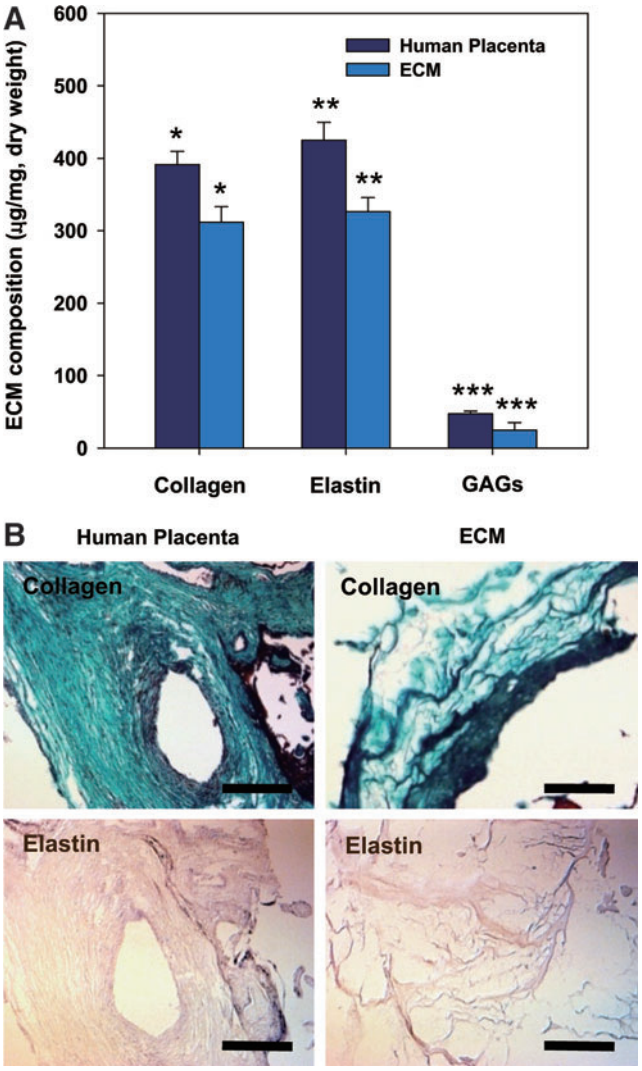

FIG. 2. **(A)** Biochemical analysis of ECM components, including acid/pepsin-soluble collagen, sulfated GAG and soluble elastin. All samples were normalized to ECM or placenta dry weight. Data are shown as mean ± standard deviation ($n = 5$) with significance at *, **, ***$p < 0.05$ between the human placenta and ECM. **(B)** ECM compositions before and after decellularization were identified using Gomori's trichrome staining (collagen, green) and orcinol-new fuchsin staining (elastin, light purple). Scale bars represent 200 μm. GAG, glycosaminoglycans. Color images available online at www.liebertpub.com/tea

wound area in the ECM sheet group was covered with a continuous epidermis. The implanted human ECM was well integrated with host cells and the space made by a partial degradation of the human ECM was replaced by the rat ECM (Fig. 8B). At 4 weeks after treatment, the wounds in the ECM sheet-implanted group were completely re-epithelialized through differentiation and organization of epidermic cells. The deposition of laminin 5 was arranged along the basement membrane zone, and keratin 15 (basal cell marker) and loricrin (hypergranulotic and hyperorthokeratotic epidermis marker) were actively expressed in suprabasal layers (Fig. 7). Moreover, a large number of hair follicles and some hairs were observed in the ECM sheet-implanted group (Fig. 6). While the restored skin of the ECM sheet-implanted group showed a similar structure to that of normal skin, the epidermis in the control group was still incomplete. These results indicate that an ECM sheet can accelerate the re-epithelialization of wounded skin.

Blood vessel formation in the wound

CD31 staining showed the vascularization of each experimental group at weeks 1 and 2 after operation and indicated a higher blood vessel density in the ECM sheet-implanted group than in the control group (Fig. 9). A large number of microvessels were observed in the ECM sheet-implanted group, and the microvessel density was much higher compared with the control group. This finding could be explained by the fact that a human placenta-derived ECM sheet contains various angiogenic factors, such as VEGF and PDGF-BB, which could activate adjacent endothelial cells and further facilitate the formation of new blood vessels in the wound.

Discussion

Decellularization techniques have been developed for preserving biochemical components, ultrastructure, and mechanical behavior, as well as reducing the antigenicity from tissues or organs.[20] Specifically, a perfusion system has been widely used as a technique for the decellularization of organs that have vasculature, such as the heart,[21] lung,[22] liver,[23] kidney,[24] and placenta.[25] In this study, the isolation and decellularization of ECM from human placentas were performed using a protocol that has been previously applied to human adipose tissue.[17,26,27] After the removal of the blood, the placentas were pulverized and centrifuged. The tissue products were subsequently decellularized using SDS and nucleases, which were effective in removing cellular components. The total collagen, elastin, and sulfated GAG were well preserved after decellularization. In particular, the placenta-derived ECM contained various bioactive molecules, including growth factors and cytokines, after decellularization. More importantly, a large amount of growth factors involved in wound healing, such as TGF-β1, bFGF, EGF, PDGF, IGF-1, and VEGF, were retained within the ECM. The wound healing process is strictly regulated by multiple growth factors, including PDGF, TGF-α, TGF-β, EGF, FGF, keratinocyte growth factor (KGF), IGF-1, tumor necrosis factor-α, interleukin (IL)-1, IL-2, and interferon.[28–30] The growth factors present in wound fluid during the healing of full-thickness cutaneous wounds act at different levels based on the time of healing; for example, TGF-β (32–1273 pg/mL), PDGF (63–1874 pg/mL), bFGF (63–512 pg/mL), VEGF (1209–1590 pg/mL), and EGF (15–111 pg/mL).[31,32] Preservation of the native ultrastructure and composition during the extraction and decellularization of the ECM from tissue is highly desirable. Similar to the retained ECM proteins, the retention of various growth factors in the decellularized ECM is an important aspect of its biological activity as an implant or scaffold material for skin tissue engineering.

The feasibility and effectiveness of a human placenta-derived ECM sheet for wound healing were investigated in a rat full-thickness cutaneous wound model. Typical approaches use a natural or synthetic scaffold in combination with various cells.[33,34] However, the manufacturing cost of

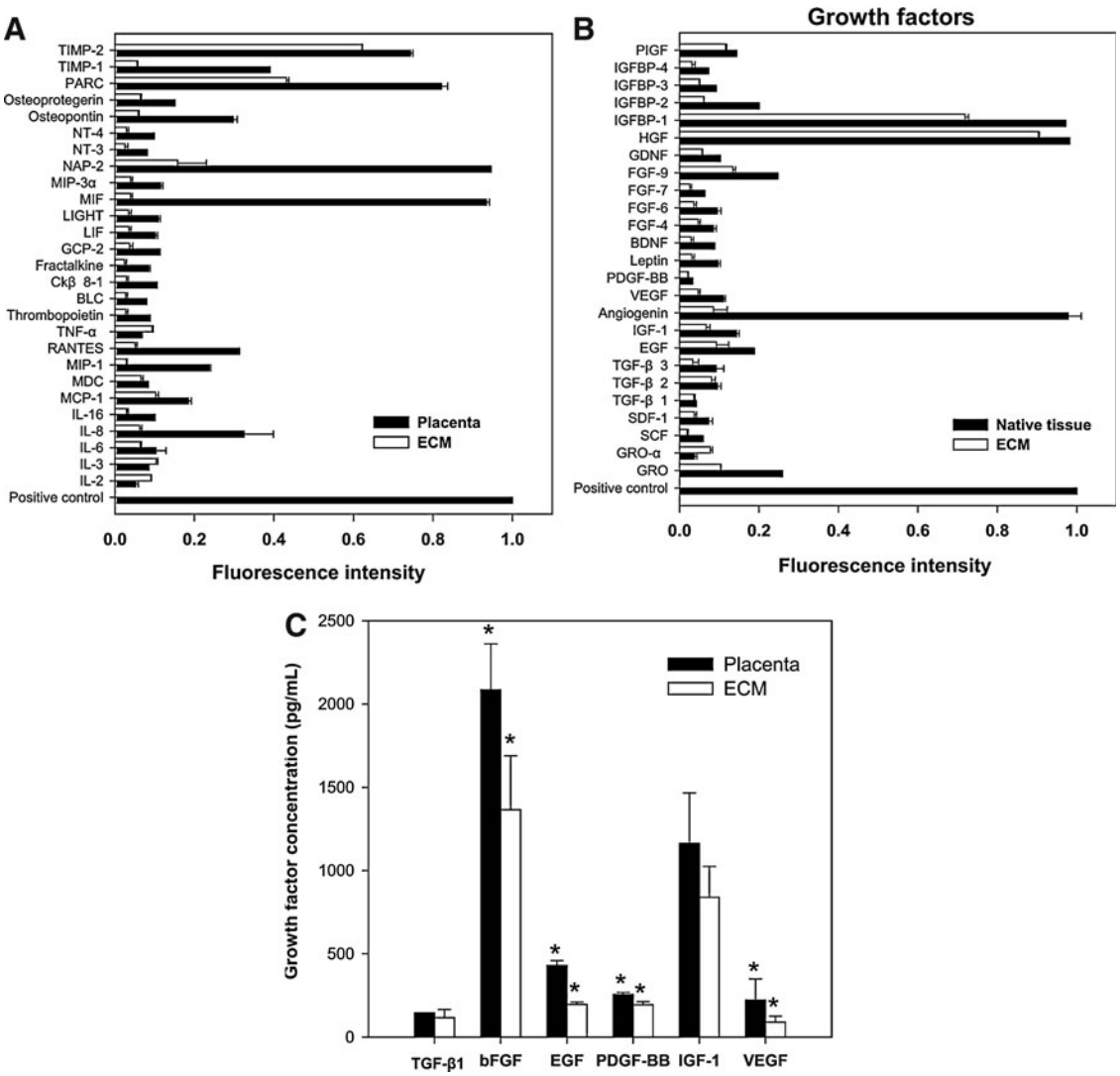

FIG. 3. Profiling of bioactive molecules and quantification of wound healing-related growth factors in human placenta and placenta-derived ECM. **(A)** Cytokines and **(B)** growth factors were arrayed on glass chip arrays containing 80 different cytokine antibodies and detected by a laser scanner using the Cy3 channel. Bioactive molecules were normalized to positive control. **(C)** Growth factors that are known to stimulate wound repair were quantified via ELISA. Data are shown as mean ± standard deviation ($n = 5$) with significance at $^*p < 0.05$ between the human placenta and ECM. BDNF, brain-derived neurotrophic factor; BLC, B-lymphocyte chemoattractant; Ckβ8, chemokine beta 8; EGF, epidermal growth factor; FGF-2, fibroblast growth factor-2; GCP, granulocyte chemotactic protein; GDNF, glial-derived neurotrophic factor; SDF, stromal cell-derived factor; GRO, growth-regulated protein; HGF, hepatocyte growth factor; IGF-1, insulin-like growth factor-1; IGFBP, IGF binding proteins; LIF, leukemia inhibitory factor; IL, interleukin; Lor, Loricrin; MIF, macrophage migration inhibitory factor; MIP, macrophage inflammatory protein; NAP, neutrophil-activating peptide; NT, neurotrophin; PARC, pulmonary and activation-regulated chemokine; PDGF, platelet-derived growth factor; PIGF, placenta growth factor; RANTES, regulated upon activation, normal T-cell expressed, and secreted; SCF, stem cell factor; TIMP, tissue inhibitor of metalloproteinase; TGF-β, transforming growth factor-β; TNF, tumor necrosis factor; VEGF, vascular endothelial growth factor.

the skin substitute containing cells is quite high and its long-term storage is difficult. In this study, decellularized placenta-derived ECM sheets were directly implanted *in vivo* without cell addition. At 3 days after implantation of the ECM sheet, macrophages were sparsely detected in the ECM sheet-implanted group, but there were no signs of an acute immunogenic response or tissue necrosis. The ECM sheet interacted effectively and protected the wound in the rat model, providing good adherence and a moist healing environment. In addition, basement membrane components and bioactive molecules in human placenta-derived ECM could play a functional part in the generation of well-structured basement membrane, regulate keratinocyte growth and differentiation, and normalize epithelial tissue architecture.[35] The degree of wound healing with ECM sheet implantation was much better than that in a control wound throughout the entire healing period. The ECM sheet implanted to a wound was well integrated into the host tissue within 7 days due to cell infiltration into the sheet. In a wound implanted with an ECM sheet, keratinocytes rapidly migrated over the wound site, and new epithelial cells formed at the wound edges. In particular, wounds implanted

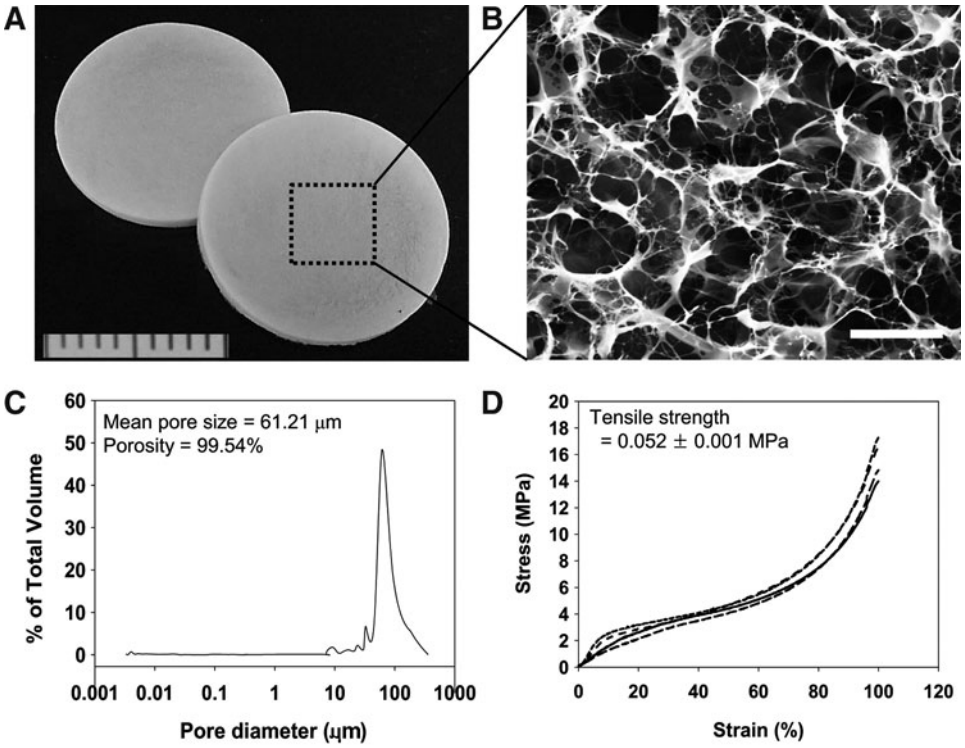

FIG. 4. Physicomechanical properties of decellularized ECM sheets. **(A)** The extracted ECM was fabricated into porous sheets. **(B)** The ECM sheets (13-mm diameter and 1-mm thickness) possessed a highly porous microstructure with a high degree of interconnectivity. Scale bar represents 50 μm. **(C)** Pore size distribution measured by a porosimeter. **(D)** Representative stress–strain curves of ECM sheets under tensile loading. Each line curve means each sample ($n=5$).

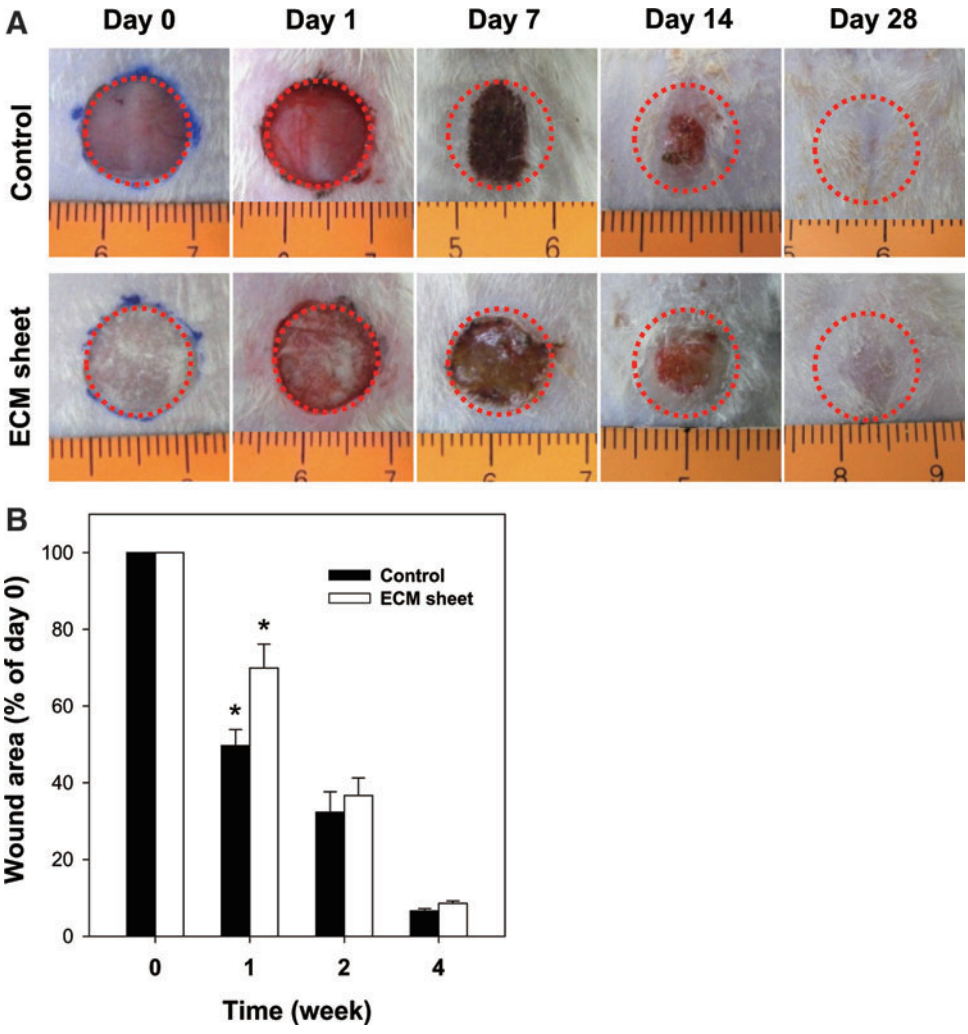

FIG. 5. The progression in healing of a full-thickness cutaneous wound treated with a human placenta-derived ECM sheet and without. **(A)** Wounds were photographed at days 0, 1, 7, 14, and 28. **(B)** The wound area was expressed as a percentage of the initial wound area at day 0. Data are shown as mean ± standard deviation ($n=6$) with significance at $^*p<0.05$. Color images available online at www.liebertpub.com/tea

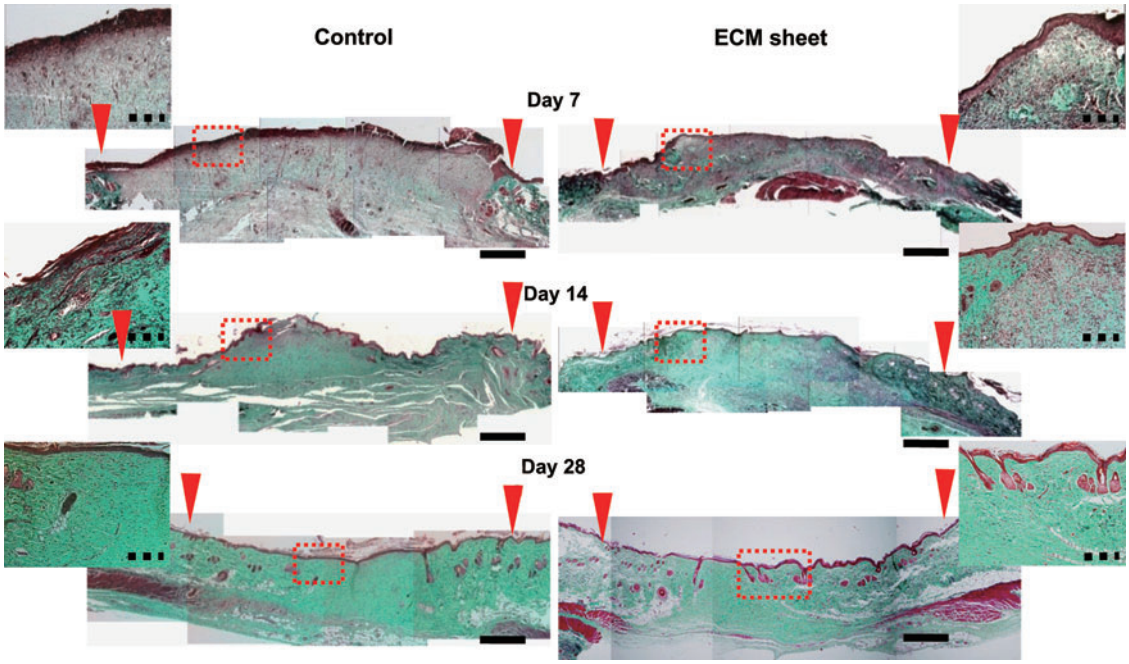

FIG. 6. Histological micrographs of wound sections implanted with an ECM sheet and without ($n=6$) at day 7, 14, and 28 after dermal excision by Gomori's trichrome staining. Wound edges are indicated by red arrows. Insets are the magnified images of the rectangles indicated, and represent the regeneration of the outer layer of the skin. Muscle, keratin, and cytoplasm: red, collagen: green, nuclei: black. Scale bars represent 2 mm (black) and 200 μm (black dotted line), respectively. Color images available online at www.liebertpub.com/tea

with an ECM sheet were rapidly remodeled within 7–14 days. At this stage, the wound implanted with an ECM sheet was covered with a continuous epidermis, and epidermal appendages were partially formed on day 14. The epidermal basement membrane layer was well formed and epidermis layers, including suprabasal, granular, and horny cell layers, were well reconstructed on day 28.

The most interesting observation was the reduction in wound contraction in the ECM sheet-implanted rats compared to that of the control rats. Wound contraction is accomplished by myofibroblasts that contain α-smooth muscle actin and mediate contractile forces produced by granulation tissue in wounds.[36,37] Although wound contraction plays a major role in the closure of a wound, the shrinkage of the

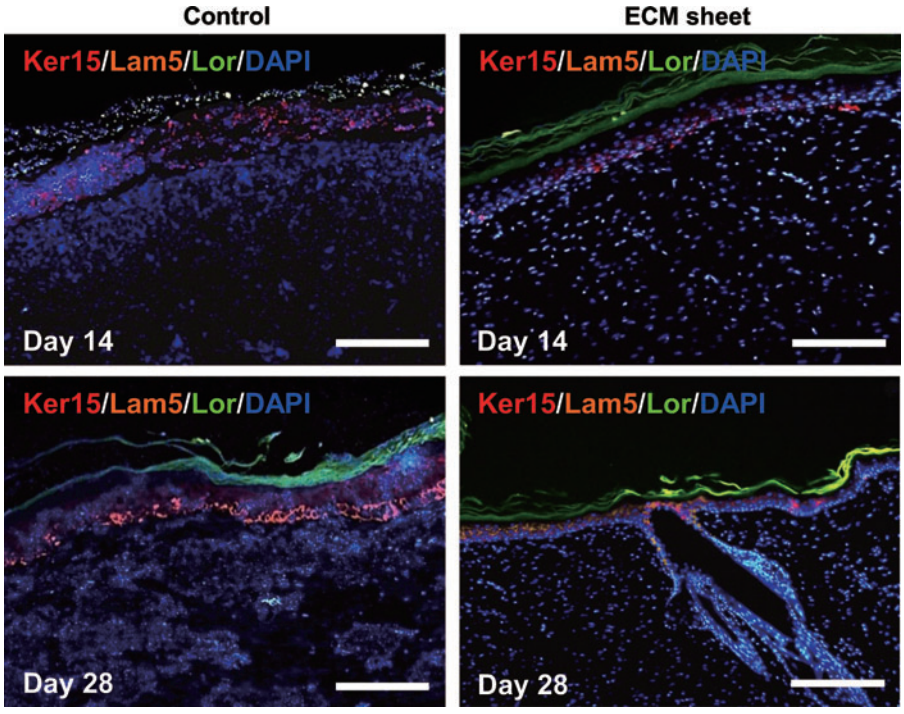

FIG. 7. Immunofluorescence staining of the wound sections implanted with an ECM sheet and without. The reconstruction of epithelia was assessed using Ker 15 (Keratin 15, red), Lam 5 (Laminin 5, orange), and Lor (Loricrin, green) on day 14 and 28. Sections were counterstained with DAPI, which stains nuclei blue. Scale bars represent 200 μm. Color images available online at www.liebertpub.com/tea

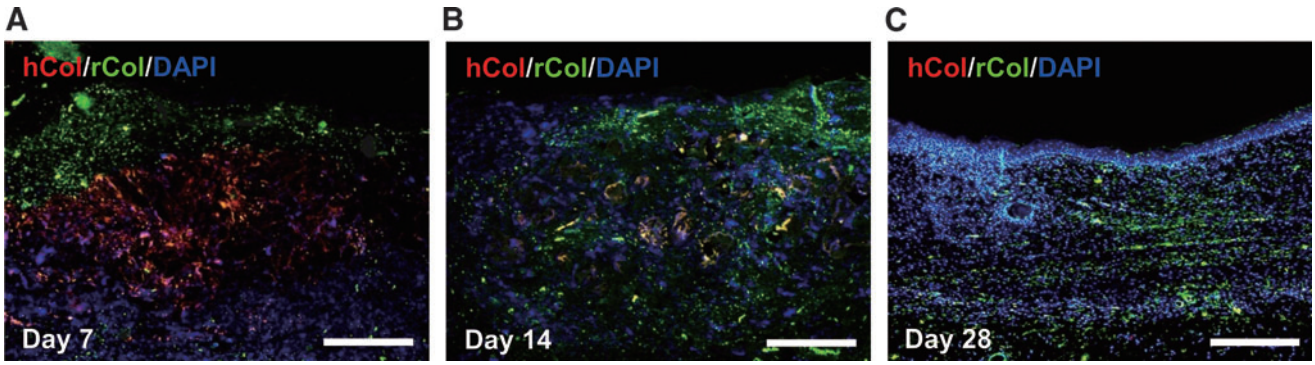

FIG. 8. The *in vivo* degradation of an ECM sheet was assessed using antibodies specific for hCol (human collagen type I, red) and rCol (rat collagen type I, green). **(A)** Day 7, **(B)** Day 14, **(C)** Day 28. Sections were counterstained with DAPI, which stains nuclei blue. Scale bars represent 200 μm. Color images available online at www.liebertpub.com/tea

healed wound can lead to a scar formation, which may cause significant functional and cosmetic morbidity.[38] The ECM sheet degraded quickly and lost its structure in about 4 weeks. The result of fast degradation without wound shrinkage in our study is quite notable. In a few previous reports,[39,40] wound contraction was much slower in wounds grafted with more stable materials, and rapid degradation of substitutes could induce fibrosis and contraction in the regeneration of the wound. In fact, the strength of the ECM sheet was significantly lower compared with rat normal skin.[19] However, the higher turnover rate of collagen in an ECM sheet may promote more rapid infiltration of host cells to the wound and more prompt wound stabilization.[41] In addition, bFGF is known to reduce wound contraction by inhibiting the phenotypic change of fibroblasts to myofibroblasts, which is likely to be involved in contraction.[42,43] Therefore, we suggest that bFGF released from an ECM sheet could contribute to the inhibition of early wound contraction.

Wound healing is a complex process involving inflammation, neovascularization, new tissue formation, and tissue remodeling.[38] At the early stage, the inflammatory response induced by ECM degradation can stimulate endothelial cell migration and induce strong proliferation of inflammatory cells, a high metabolic rate, and a low oxygen content in the regenerated tissues, which are supposed to promote neovascularization.[44,45] Moreover, angiogenic growth factors released by the inflammatory cells, such as bFGF, PDGF, TGF-β1, and VEGF contribute to neovascularization by promoting the formation of new capillaries and stimulating the proliferation of endothelial cells, migration, and tube formation.[28] In this study, a human placenta-derived ECM sheet containing various endogenous growth factors showed a significant neovascularization ability compared to that of the controls *in vivo*. On day 7, a large number of microvessels were observed in the ECM sheet implanted wound, whereas no microvessels were observed in the control wound. On day

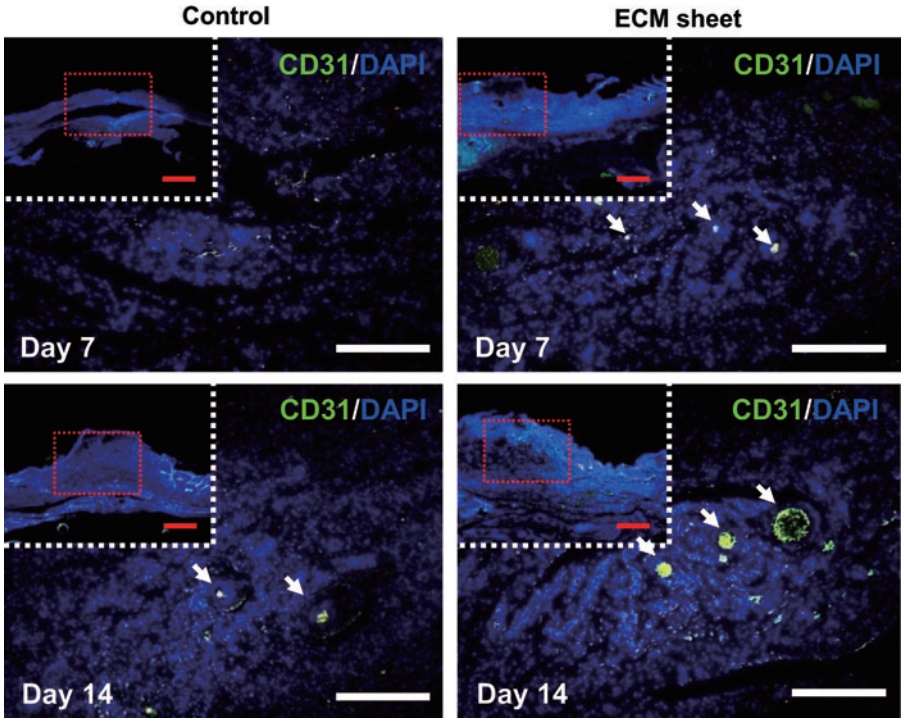

FIG. 9. Distribution and density of newly formed blood vessels were assessed using a CD31 (green) for rat endothelial cells on day 7 and 14. Arrows denote areas of magnified images and show the formation of newly blood vessels. Sections were counterstained with DAPI, which stains nuclei blue. Scale bars represent 1 mm (red) and 200 μm (white). Color images available online at www.liebertpub.com/tea

14, microvessels were found in all wounds, but the microvessel size in the ECM sheet-implanted wound was more distinctive and the density was higher compared with the control. Our results indicate that the secretion of endogenous growth factors from an ECM sheet may lead to an early and well-developed neovascularization.

Conclusions

In this study, human placenta-derived ECM sheets composed of various ECM components and endogenous growth factors were developed as a biological scaffold for skin tissue engineering. Human ECM sheets were fabricated from human placentas through pulverization, decellularization, and freeze-drying. Our findings suggest that human placenta-derived ECM sheets could effectively promote the migration of keratinocytes and epithelial cells, as well as neovascularization due to a combination of physicomechanical and compositional properties, thereby improving the quality of wound healing.

Acknowledgments

This work was supported by the Basic Science Research Program (Grant No. 2009-0075546) and the Bio and Medical Technology Development Program (Grant No. 2011-0019774) through the National Research Foundation of Korea (NRF) funded by the Korean government (MEST). This work (Grants No. 00046001) was also supported by Business for Academic-Industrial Cooperative Establishments funded Korea Small and Medium Business Administration in 2011.

Disclosure Statement

No competing financial interests exist.

References

1. MacNeil, S. Progress and opportunities for tissue-engineered skin. Nature **445,** 874, 2007.
2. Shevchenko, R.V., James, S.L., and James, S.E. A review of tissue-engineered skin bioconstructs available for skin reconstruction. J R Soc Interface **7,** 229, 2010.
3. Clark, R.A., Ghosh, K., and Tonnesen, M.G. Tissue engineering for cutaneous wounds. J Invest Dermatol **127,** 1018, 2007.
4. Choi, J.S., Yang, H.J., Kim, B.S., Kim, J.D., Kim, J.Y., Yoo, B., *et al.* Human extracellular matrix (ECM) powders for injectable cell delivery and adipose tissue engineering. J Control Release **139,** 2, 2009.
5. Liao, J., Joyce, E.M., and Sacks, M.S. Effects of decellularization on the mechanical and structural properties of the porcine aortic valve leaflet. Biomaterials **29,** 1065, 2008.
6. Zhang, X., Deng, Z., Wang, H., Yang, Z., Guo, W., Li, Y., *et al.* Expansion and delivery of human fibroblasts on micronized acellular dermal matrix for skin regeneration. Biomaterials **30,** 2666, 2009.
7. Wildman, D.E. Review: toward an integrated evolutionary understanding of the mammalian placenta. Placenta **32,** S142, 2011.
8. Chen, C.P., and Aplin, J.D. Placental extracellular matrix: gene expression, deposition by placental fibroblasts and the effect of oxygen. Placenta **24,** 316, 2003.
9. Forbes, K., and Westwood, M. Maternal growth factor regulation of human placental development and fetal growth. J Endocrinol **207,** 1, 2010.
10. Hopkinson, A., Shanmuganathan, V.A., Gray, T., Yeung, A.M., Lowe, J., James, D.K., *et al.* Optimization of amniotic membrane (AM) denuding for tissue engineering. Tissue Eng Part C Methods **14,** 371, 2008.
11. Lopez-Espinosa, M.J., Silva, E., Granada, A., Molina-Molina, J.M., Fernandez, M.F., Aguilar-Garduño, C., *et al.* Assessment of the total effective xenoestrogen burden in extracts of human placentas. Biomarkers **14,** 271, 2009.
12. Hong, J.W., Lee, W.J., Hahn, S.B., Kim, B.J., and Lew, D.H. The effect of human placenta extract in a wound healing model. Ann Plast Surg **65,** 96, 2010.
13. De, D., Chakraborty, P.D., and Bhattacharyya, D. Regulation of trypsin activity by peptide fraction of an aqueous extract of human placenta used as wound healer. J Cell Physiol **226,** 2033, 2011.
14. Schenke-Layland, K., Vasilevski, O., Opitz, F., König, K., Riemann, I., Halbhuber, K.J., *et al.* Impact of decellularization of xenogeneic tissue on extracellular matrix integrity for tissue engineering of heart valves. J Struct Biol **143,** 201, 2003.
15. Balachandran, K., Konduri, S., Sucosky, P., Jo, H., and Yoganathan, A.P. An *ex vivo* study of the biological properties of porcine aortic valves in response to circumferential cyclic stretch. Ann Biomed Eng **34,** 1655, 2006.
16. Romanowicz, L., and Sobolewski, K. Extracellular matrix components of the wall of umbilical cord vein and their alterations in pre-eclampsia. J Perinat Med **28,** 140, 2000.
17. Choi, J.S., Yang, H.J., Kim, B.S., Kim, J.D., Lee, S.H., Lee, E.K., *et al.* Fabrication of porous extracellular matrix scaffolds from human adipose tissue. Tissue Eng Part C Methods **16,** 387, 2010.
18. Chen, Q.-Z., Harding, S.E., Ali, N.N., Lyon, A.R., and Boccaccini, A.R. Biomaterials in cardiac tissue engineering: ten years of research survey. Mat Sci Eng R **59,** 1, 2008.
19. Ozyazgan, I., Liman, N., Dursun, N., and Güneş, I. The effects of ovariectomy on the mechanical properties of skin in rats. Maturitas **43,** 65, 2002.
20. Crapo, P.M., Gilbert, T.W., and Badylak, S.F. An overview of tissue and whole organ decellularization processes. Biomaterials **32,** 3233, 2011.
21. Ott, H.C., Matthiesen, T.S., Goh, S.K., Black, L.D., Kren, S.M., Netoff, T.I., *et al.* Perfusion-decellularized matrix: using nature's platform to engineer a bioartificial heart. Nat Med **14,** 213, 2008.
22. Petersen, T.H., Calle, E.A., Zhao, L., Lee, E.J., Gui, L., Raredon, M.B., *et al.* Tissue-engineered lungs for *in vivo* implantation. Science **329,** 538, 2010.
23. Uygun, B.E., Soto-Gutierrez, A., Yagi, H., Izamis, M.L., Guzzardi, M.A., Shulman, C., *et al.* Organ reengineering through development of a transplantable recellularized liver graft using decellularized liver matrix. Nat Med **16,** 814, 2010.
24. Ross, E.A., Williams, M.J., Hamazaki, T., Terada, N., Clapp, W.L., Adin, C., *et al.* Embryonic stem cells proliferate and differentiate when seeded into kidney scaffolds. J Am Soc Nephrol **20,** 2338, 2009.
25. Flynn, L., Semple, J.L., and Woodhouse, K.A. Decellularized placental matrices for adipose tissue engineering. J Biomed Mater Res A **79,** 359, 2006.
26. Choi, J.S., Kim, B.S., Kim, J.Y., Kim, J.D., Choi, Y.C., Yang, H.J., *et al.* Decellularized extracellular matrix derived from human adipose tissue as a potential scaffold for allograft tissue engineering. J Biomed Mater Res A **97,** 292, 2011.

27. Choi, J.S., Kim, B.S., Kim, J.D., Choi, Y.C., Lee, E.K., Park, K., *et al. In vitro* expansion of human adipose-derived stem cells in a spinner culture system using human extracellular matrix powders. Cell Tissue Res **345,** 415, 2011.
28. Werner, S., and Grose, R. Regulation of wound healing by growth factors and cytokines. Physiol Rev **83,** 835, 2003.
29. Clark, R.A. Synergistic signaling from extracellular matrix-growth factor complexes. J Invest Dermatol **128,** 1354, 2008.
30. Mauviel, A. Transforming growth factor-β signaling in skin: stromal to epithelial cross-talk. J Invest Dermatol **129,** 7, 2009.
31. Baker, E.A., Kumar, S., Melling, A.C., Whetter, D., and Leaper, D.J. Temporal and quantitative profiles of growth factors and metalloproteinases in acute wound fluid after mastectomy. Wound Repair Regen **16,** 95, 2008.
32. Vogt, P.M., Lehnhardt, M., Wagner, D., Jansen, V., Krieg, M., and Steinau, H.U. Determination of endogenous growth factors in human wound fluid: temporal presence and profiles of secretion. Plast Reconstr Surg **102,** 117, 1998.
33. Dubé, J., Rochette-Drouin, O., Lévesque, P., Gauvin, R., Roberge, C.J., Auger, F.A., *et al.* Restoration of the transepithelial potential within tissue-engineered human skin *in vitro* and during the wound healing process *in vivo*. Tissue Eng Part A **16,** 3055, 2010.
34. Ma, K., Liao, S., He, L., Lu, J., Ramakrishna, S., and Chan, C.K. Effects of nanofiber/stem cell composite on wound healing in acute full-thickness skin wounds. Tissue Eng Part A **17,** 1413, 2011.
35. Stoker, A.W., Streuli, C.H., Martins-Green, M., and Bissell, M.J. Designer microenvironments for the analysis of cell and tissue function. Curr Opin Cell Biol **2,** 864, 1990.
36. Eldardiri, M., Martin, Y., Roxburgh, J., Lawrence-Watt, D.J., and Sharpe, J.R. Wound contraction is significantly reduced by the use of microcarriers to deliver keratinocytes and fibroblasts in an in vivo pig model of wound repair and regeneration. Tissue Eng Part A **18,** 587, 2012.
37. Darby, I.A., and Hewitson, T.D. Fibroblast differentiation in wound healing and fibrosis. Int Rev Cytol **257,** 143, 2007.
38. Gurtner, G.C., Werner, S., Barrandon, Y., and Longaker, M.T. Wound repair and regeneration. Nature **453,** 314, 2008.
39. Powell, H.M., and Boyce, S.T. Wound closure with EDC cross-linked cultured skin substitutes grafted to athymic mice. Biomaterials **28,** 1084, 2007.
40. Wong, V.W., Rustad, K.C., Galvez, M.G., Neofytou, E., Glotzbach, J.P., Januszyk, M., *et al.* Engineered pullulan-collagen composite dermal hydrogels improve early cutaneous wound healing. Tissue Eng Part A **17,** 631, 2011.
41. Arora, P.D., Narani, N., and McCulloch, C.A. The compliance of collagen gels regulates transforming growth factor-beta induction of alpha-smooth muscle actin in fibroblasts. Am J Pathol **154,** 871, 1999.
42. Numata, Y., Terui, T., Okuyama, R., Hirasawa, N., Sugiura, Y., Miyoshi, I., *et al.* The accelerating effect of histamine on the cutaneous wound-healing process through the action of basic fibroblast growth factor. J Invest Dermatol **126,** 1403, 2006.
43. Hinz, B. Formation and function of the myofibroblast during tissue repair. J Invest Dermatol **127,** 526, 2007.
44. Eming, S.A., Krieg, T., and Davidson, J.M. Inflammation in wound repair: molecular and cellular mechanisms. J Invest Dermatol **127,** 514, 2007.
45. Tufro-McReddie, A., Norwood, V.F., Aylor, K.W., Botkin, S.J., Carey, R.M., and Gomez, R.A. Oxygen regulates vascular endothelial growth factor-mediated vasculogenesis and tubulogenesis. Dev Biol **183,** 139, 1997.

Address correspondence to:
Yong Woo Cho, PhD
Department of Chemical Engineering and Bionanotechnology
Hanyang University
Ansan, Gyeonggi-do 426-791
Korea

E-mail: ywcho7@hanyang.ac.kr

Received: December 26, 2011
Accepted: August 13, 2012
Online Publication Date: September 20, 2012